Optically excited nanoscale ultrasonic transducers

Richard J. Smith,[a] Fernando Perez Cota, Leonel Marques, and Xuesheng Chen
Electrical Systems and Optics Research Division, University of Nottingham, University Park, Nottingham, NG7 2RD, United Kingdom

Ahmet Arca
Department of Electric and Electronic Engineering, Faculty of Architecture and Engineering, European University of Lefke, Gemikonagi, Mersin 10, Turkey

Kevin Webb
Electrical Systems and Optics Research Division, University of Nottingham, University Park, Nottingham, NG7 2RD, United Kingdom

Jonathon Aylott
School of Pharmacy, University of Nottingham, United Kingdom

Micheal G. Somekh
Department of Electronic and Information Engineering, The Hong Kong Polytechnic University, Kowloon, Hong Kong

Matt Clark
Electrical Systems and Optics Research Division, University of Nottingham, University Park, Nottingham, NG7 2RD, United Kingdom

In order to work at higher ultrasonic frequencies, for instance, to increase the resolution, it is necessary to fabricate smaller and higher frequency transducers. This paper presents an ultrasonic transducer capable of being made at a very small size and operated at GHz frequencies. The transducers are activated and read optically using pulsed lasers and without physical contact between the instrumentation and the transducer. This removes some of the practical impediments of traditional piezo-electric architectures (such as wiring) and allows the devices to be placed immediately on or within samples, reducing the significant effect of attenuation which is very strong at frequencies above 1 GHz. The transducers presented in this paper exploit simultaneous optical and mechanical resonances to couple the optical input into ultrasonic waves and vice versa. This paper discusses the mechanical and optical design of the devices at a modest scale (a few μm) and explores the scaling of the transducers toward the sub-micron scale. Results are presented that show how the transducers response changes depending on its local environment and how the resonant frequency shifts when the transducer is loaded by a printed protein sample. © 2015 Acoustical Society of America. [http://dx.doi.org/10.1121/1.4904487]

Pages: 219–227

I. INTRODUCTION

Ultrasonics offers an intriguing route to high resolution imaging and measurement because the speed of sound is ~5 orders of magnitude lower than the speed of light. For the same wavelength this makes the frequency of sound with optical scale wavelengths in the GHz range. Furthermore, many small scale objects of interest (such as cells) exhibit very little intrinsic optical contrast but may offer useful contrast for ultrasound.

There are significant practical problems to implementing ultrasound in the GHz region using the sort of piezo-electric transducer technology that is ubiquitous in the MHz region, for instance, the attenuation of ultrasound is extremely high in the GHz region [1900 dB mm^{-1} at 4.4 GHz (Ref. 1)], making it difficult to use any form of couplant, the small size of the transducers required at multi GHz frequencies makes it a considerable technical challenge just to provide electrical wiring to the transducer, and the electronics to drive and detect the multi GHz analog signals are expensive.

It is possible to overcome these problems but as the frequency increases beyond a GHz increasingly extreme measures are required, for instance Quate's group[1,2] used 15 μm focal length acoustic lenses and liquid helium as a couplant to perform acoustic microscopy in the low GHz range.

It is also possible to generate and detect ultrasound in the GHz region using picosecond laser ultrasonics. Here short pulsed lasers are used to generate and detect the ultrasound. This arrangement overcomes some of these practical problems associated with piezo-electric transducers because: There is no need for a couplant, the lasers provide access to high speeds, and the pump-probe architecture removes the need for extremely fast electronics. This technique has been used to investigate the optical and mechanical properties of

[a] Author to whom correspondence should be addressed. Electronic mail: richard.j.smith@nottingham.ac.uk

thin films,[3] semi-conductors,[4] novel materials,[5] liquids,[6] and recently picosecond laser ultrasonics has been shown to be possible on biological cells.[7,8] In these techniques the frequency of the ultrasound generated depends on the optical absorption in the sample and the frequency content of the laser pulses and can reach over 100 GHz. However, the minimum lateral extent or ultrasound beam size is usually determined by the optical spot size which limits the lateral resolution despite the ultrasonic wavelength being significantly shorter than the optical wavelength. Furthermore the efficiency of optical generation and detection can be low, resulting in the need to use a relatively large amount of laser energy and averaging of the signal to overcome the low signal-to-noise level.

In this paper, we introduce an optically driven ultrasonic transducer that acts simultaneously as an optical and ultrasonic resonator and is designed so that it couples from light to ultrasound and vice versa efficiently.

Using a transducer, rather than the sample (as is commonly used in picosecond ultrasonic systems) to generate and detect the ultrasound allows the signal-to-noise ratio to be improved which, in turn, improves the speed of measurement and enables imaging. Although not demonstrated in this paper this technique has the potential to produce ultrasound with a smaller lateral extent than the optical wavelength by using curved transducers or those with a sub-optical wavelength size.

There has been much interest in micro[9,10] and nano[11–13] sized structures, for both the measurement of their inherent properties and their potential for many different sensing applications. The structures studied to date range in shape and size and include rings,[11] rods,[12] spheres,[9] shells,[13] and cylinders/fibers.[10] These have been investigated for their optical, mechanical, and plasmonic properties which has led to a number of possible sensing applications, for example, ultrasensitive mass detection,[14] biosensing,[15] and single molecule sensitivity surface enhanced Raman spectroscopy.[16] It is also possible to place small structures at this scale directly into or onto cells.[17,18]

Using optical resonances to improve the detection of ultrasound has been known for some time, for example, the trade-off between sensitivity, ultrasonic detection bandwidth, and the structural properties of an etalon was discussed by Ref. 19, Fabry-Pérot detectors[20] have been used in photo acoustic measurements with an etalon substrate for the detection of low frequency acoustic waves[21,22] and at high frequencies with an air gap cavity formed between a reflector and the sample being studied.[23] The transducers presented here are small structures that form zero-order Fabry-Pérot cavities. They are designed to be as thin as possible and we also make use of the mechanical resonance of the devices for generating high frequency ultrasound.

There are a number of different approaches to produce these small scale structures and we introduce one method for building these devices. At this time the devices are nanoscale in one dimension only and we will discuss methods to reduce the size of the devices to be nanoscale in all dimensions. The devices have been extensively modeled so that the parameters governing their behavior could be tuned to produce a device that is effective from a mechanical and optical point of view. We have produced various different sizes of devices which have been measured in a pump probe picosecond ultrasound system.[24,25]

This paper describes the optical (Sec. II A) and mechanical (Sec. II B) design and operation of the devices and how to choose the correct parameters to get optimal performance. Then follows a description of the fabrication process (Sec. II C), the experimental setup (Sec. III A), the results obtained imaging a protein coating (Sec. III C), and a discussion of the future use and development of the transducers (Sec. IV).

II. DESIGN AND FABRICATION OF THE TRANSDUCERS

The structure of the devices is shown schematically in Fig. 1. They are comprised of a sandwich structure of partially transparent metal layers around an optically transparent filling. The transducers exploit the optical resonances within the layers which form a zero-order Fabry-Pérot interferometer.[20,26]

The optical design of the transducers is such that they strongly absorb at one wavelength of light (λ_{pump}) (making them efficient thermoelastic generators of elastic waves[27]) and, more crucially, strongly reflect at a second wavelength (λ_{probe}). The thickness of the layers is chosen so that the reflectivity of the transducer at λ_{probe} sits around half way up one of the optically resonant reflectivity peaks (see Fig. 2 and Sec. II A) and changes in the thicknesses of the layers, therefore changing the reflectivity of the transducer.

As a result when illuminated with a short (ps) pulse of light at λ_{pump} they generate elastic waves and when illuminated by a short (ps) pulse of light at λ_{probe} the reflected light intensity indicates any (instantaneous) change in size (caused by mechanical vibration).

The sensitivity of the transducers depends on how the energy of the two optical beams is absorbed and reflected at these two optical wavelengths which is determined by the
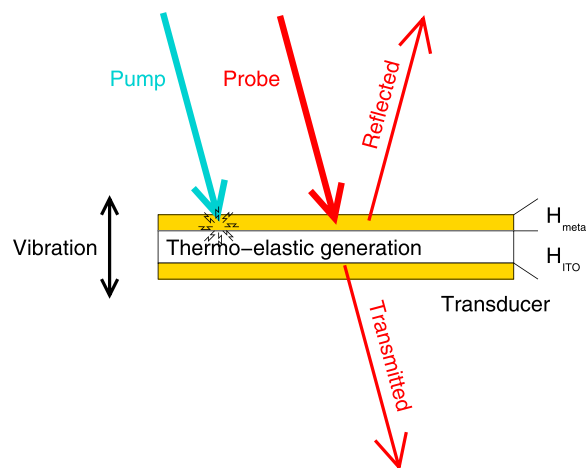

FIG. 1. (Color online) Schematic of the transducer design showing pump and probe laser beams, vibration, and critical dimensions H_{metal} and H_{ITO}; the top and bottom layers are assumed to be identical, typically the construction is gold:ITO:gold with dimensions $H_{metal} \sim 30$ nm and $H_{ITO} \sim 150$ nm. The construction is chosen such that the pump beam is strongly absorbed and the probe beam is strongly reflected (see text).
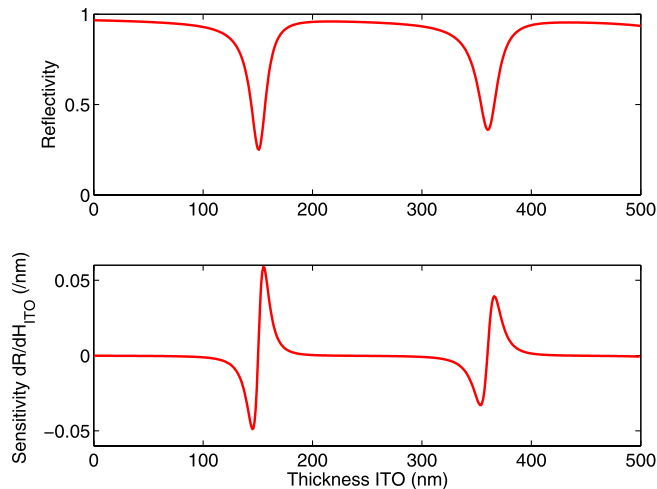
FIG. 2. (Color online) Modeling the optical reflection coefficient (top) and detection sensitivity coefficient (bottom) from transducer vs change in H_{ITO}. For this graph the top and bottom layers are 30 nm gold and the optical wavelength is 780 nm.

layer structure, layer thicknesses, and materials used to fabricate them.

From a mechanical point of view the transducers form a simple plate structure which will resonate when excited and, if in contact with another medium, radiate elastic waves. The resonant frequency is determined by the same parameters as the sensitivity, which needs to be properly combined to optimize the design of the transducer. The frequency is also strongly influenced by coupling to external media.

The devices presented here can all be adequately modeled using simple one-dimensional approximations because the lateral size of the transducer and the lateral size of the pump-beam excitation spot are significantly greater than the thickness of the transducer. Where these conditions are not met the modeling becomes significantly more complicated, typically requiring three-dimensional (3D) numerical models to describe the optical and mechanical behavior of the transducers.

For our experiment the two optical wavelengths (390 and 780 nm) are determined by our laser system and this governs the choice of materials and layer thicknesses. Even so, as can be seen in Secs. II A and II B there are a large range of possible layer thicknesses that can be exploited to allow some degree of freedom with which to tune the mechanical resonances. For a larger range of mechanical tuning it would be possible to use higher order optical resonances but at the expense of tighter fabrication tolerances.

A. Optical design and modeling

The devices operate in a manner similar to that of a Fabry-Pérot interferometer. The layer structure is designed so that the top and bottom metal layers are partial reflectors (Fig. 1). Part of the probe beam incident on the transducer is transmitted into the cavity formed between the metal layers and is resonantly reflected (and transmitted) by the structure. This is illustrated in Fig. 2 for a typical construction of gold layers around a core of indium tin oxide (ITO). The top graph shows the reflectivity of normal incident light at

780 nm as a function of the ITO thickness. The reflectivity shows distinct, sharp dips and by carefully fabricating the transducer with a core thickness corresponding to a thickness half way down one of these dips then any change in the thickness (for instance, caused by an elastic wave compressing the structure) leads to a change in the reflectivity. This is shown in the lower graph which plots dR/dH_{ITO} or the sensitivity of the transducer.

In addition to reflecting and transmitting light the transducer also absorbs some light leading to localized heating. Through a careful choice of materials, optical wavelengths and layer structures, it is possible to arrive at a design where the absorption at λ_{pump} and the sensitivity at λ_{probe} are both high. This produces a transducer that is both an efficient thermoelastic generator and a sensitive detector.

Figure 3 shows a plot of the sensitivity of a gold:ITO:gold structure against H_{metal} and H_{ITO} calculated by considering the Fresnel reflection coefficient of the structure[20] at $\lambda_{\mathrm{probe}} = 780$ nm. A similar plot can be made for the absorption at $\lambda_{\mathrm{pump}} = 390$ nm which shows that if $H_{\mathrm{metal}} > 5$ nm the absorption is uniformly high at around 0.6 by virtue of the high absorption coefficient of gold at this wavelength.

The calculation of the Fresnel reflection coefficient assumes the structure is of infinite width but is a fair approximation provided the width is greater than the optical wavelength.

The effect the stress has on the refractive indices of the materials (the photoelastic effect, commonly used detection mechanism in picosecond ultrasonics) is *not* considered as it is considerably weaker than the change in reflectivity caused by optical cavity changes.[27,28] Estimating the relative sensitivity of the transducer compared with photoelastic detection gives an improvement of over 2 orders of magnitude for an optimal gold:ITO:gold transducer compared with photoelastic detection on (commonly used) chrome.[29]
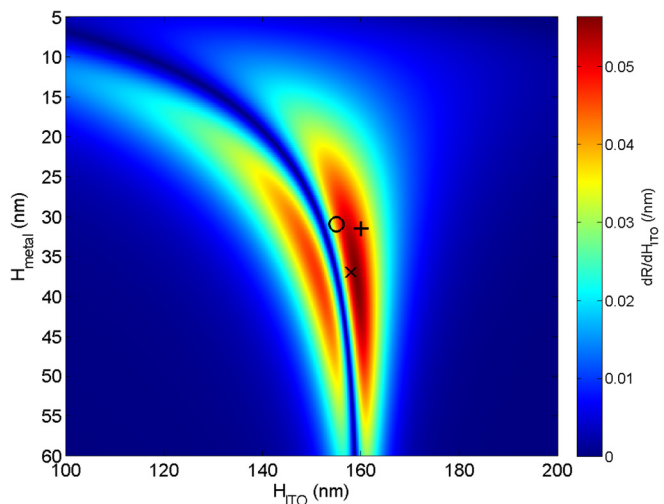

FIG. 3. (Color online) Modeling the detection sensitivity as a function of H_{metal} and H_{ITO} for a gold:ITO:gold transducer at $\lambda_{\mathrm{probe}} = 780$ nm. The position of the greatest signal is marked with an "×." However, because the reflectivity is also varying, this point differs from the point of greatest signal-to-noise ratio which is marked with a, "○." The (approximate) position of the transducers presented here is shown by a "+." A similar plot for absorption (not shown here) for $\lambda_{\mathrm{pump}} = 390$ nm shows a uniformly high optical absorption of around 0.6 provided $H_{\mathrm{metal}} > 5$ nm.

From Fig. 3 we can see that for a gold:ITO:gold sandwich the best sensitivity is achieved with a $\sim$30 nm gold layer and $\sim$155 nm ITO layer. Crucially, this region of good sensitivity is reasonably broad in both H_{metal} and H_{ITO}, meaning that the device fabrication tolerances are acceptable.

One thing to note is that the probe laser pulse is not a single wavelength as assumed above; it contains a range of wavelengths due to the short pulse width. For example, our 150 fs pulse has a full width at half-maximum of approximately 5 nm. Whether this has an effect on the sensitivity of the cavity depends on both the optical bandwidth and the sharpness of the cavity peak (the finesse). For the device described above the bandwidth of the cavity response is much wider than the optical bandwidth (47 nm vs 5 nm, respectively). This means that the slope of the response for each wavelength present in the pulse is essentially the same, and so the sensitivity is unaffected. However, if the finesse was higher, e.g., in the 100–300 range as is more typical for lower frequency ultrasound detection,[19] then this would no longer hold as the different wavelengths would see gradients of differing size and more importantly of opposite signs, thus the sensitivity would drop off rapidly.

B. Mechanical design and modeling

The biggest constraint on the design of the transducers is meeting the optical conditions for generation and detection. Within this framework there is a considerable scope for tuning the mechanical response of the transducers. In this paper the ultrasonic frequency was not critical so the transducers were designed to give good optical responses and good optical tolerances. However we modeled the structures to determine their expected frequencies of oscillation and (change in) response to the external media.

Since the structures have a number of boundaries and the excitation is performed thermoelastically using an optical source the modeling of the vibration does not lend itself to easy analytical analysis. Instead we have modeled these devices using finite element modeling (FEM) and used a coupled optical-thermal-mechanical model to predict their behavior when excited by a short laser pulse. Since the devices presented in this paper are a few μm wide and, in any event, excited with a laser spot at least several times the thickness of the transducers, the modeling was performed in one dimension.

Modeling the optical absorption at 390 nm shows that it takes place predominantly in the metal layers (especially the top metal layer) because of the high absorption coefficient of gold.

Consequently the FEM models the excitation of the pump pulse as an injection of heat into the metal layers. The model then computes the temperature changes, stress, and motion of the structure.

Finally, the effect on the movement of the structure on the reflectivity of the pump beam can be calculated by computing the Fresnel reflection coefficients as described in Sec. II A.

The result from the mechanical model for a gold:ITO:gold structure on a glass substrate where the gold layers are 31 and 32 nm thick and the ITO is 160 nm thick is

shown in Fig. 4 (the layer thicknesses were measured from experimentally fabricated transducers and used in the models). The plotted value is the difference in displacement between the top and bottom metal layers with time. We observe a decaying oscillating signal composed of three or four main frequency components. The frequencies that are present are related (although not exactly) to the round trip times of the acoustic waves through the different parts of the structure. The signal decays quickly as the acoustic impedance mismatch between the gold and the glass layers is low and energy is quickly radiated into the glass substrate.

By placing the transducer on a polymer layer [in this case polystyrene (PS)] which acts as a buffer between the transducer and the glass substrate, the oscillations can be extended over a much longer time period because the decay (through radiated energy) is much lower. This is shown in Fig. 5 for the same structure as Fig. 4 but with a PS (nominally $\sim$1 μm thick) layer between the transducer and the glass substrate.

This model can be used to predict the resonant frequencies of the transducers according to their construction and layer thicknesses (see Fig. 6) and if there is a need to design for a particular frequency this, together with the optical design constraints discussed in Sec. II A, can be used to select the appropriate materials, construction, and layer thicknesses. For the simple devices presented here it is feasible to tune their frequency response over a wide range ($\sim$5–20 GHz for our single wavelength laser).

C. Fabrication of the transducers

We have approached the fabrication of these transducers from a "top down" method by building a large patterned surface with photolithography techniques and then laying down the films over the whole substrate one at a time. The transducers can then be liberated from the substrate and then encapsulated and functionalized. In this paper the structures
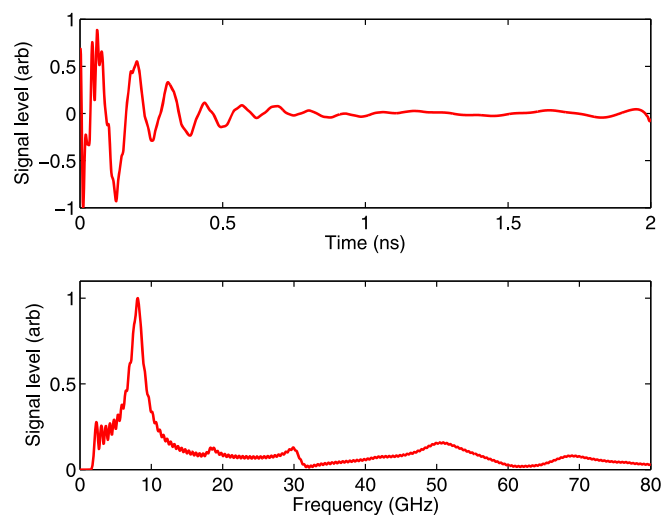

FIG. 4. (Color online) FEM simulation of the mechanical response of a 31:160:32 nm gold:ITO:gold transducer directly attached to a glass substrate. The time trace (top) shows the separation of the top and bottom metal layers. The frequency response (bottom) shows a fundamental resonance around 10 GHz and secondary resonances at $\sim$30 and $\sim$50 GHz.
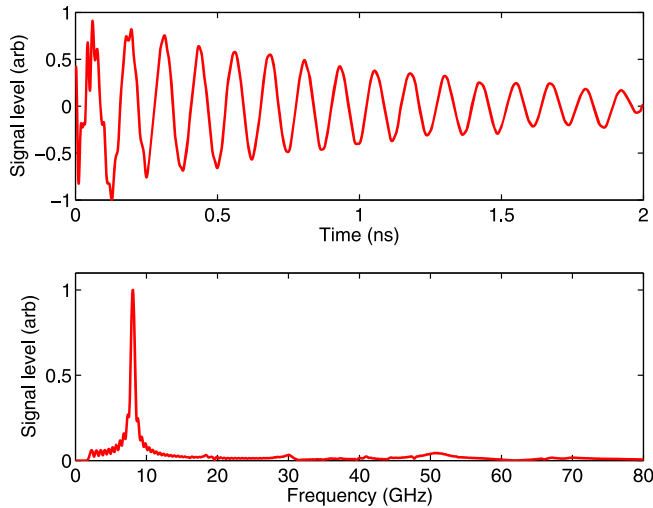
FIG. 5. (Color online) FEM simulation of the mechanical response of the structure shown in Fig. 4 with the addition of a PS layer between the transducer and glass substrate. This buffers the transducer, reducing the radiation of elastic waves into the substrate and allowing it to oscillate longer. The time trace (top) and frequency response (bottom) shows a much higher Q of oscillation.

are made from gold metal outer layers and a filling of ITO (see Fig. 7).

We have used standard photolithography techniques to fabricate patterned substrates to produce transducers with lateral sizes of 5, 10, 15, and 20 μm. The layers are deposited using a direct current sputter coater which governs the choice of the dielectric material used—ITO (Ref. 30). With alternative deposition techniques a wider range of dielectrics can be used.

The thickness of the films during fabrication is controlled using a conventional film thickness monitor in the sputterer but to aid the calibration and enhance the accuracy
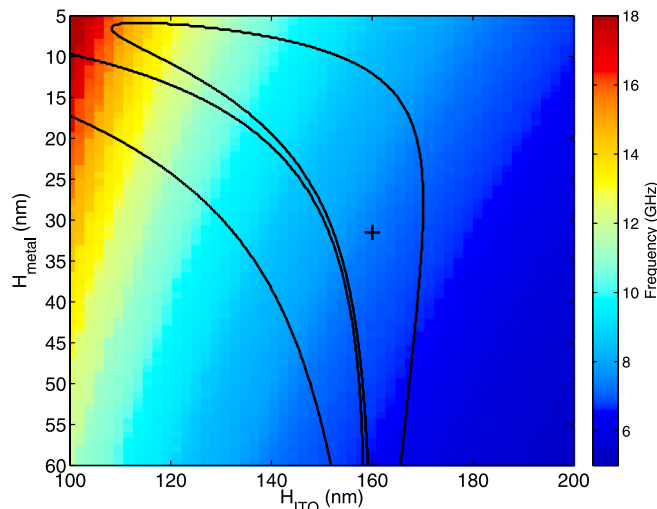

FIG. 6. (Color online) Simulation of the mechanical resonance showing the frequency of the first mechanical resonance vs H_{metal} and H_{ITO}, the overlay is a contour plot showing the usable optical detection region from Fig. 3. It can be seen that the frequency can be tuned over a wide range (6–18 GHz for this design). By combining this with Fig. 3 regions of high sensitivity (the regions inside the black lines) may be found over a wide frequency range. The + marks the position of the transducers experimentally demonstrated in this paper.
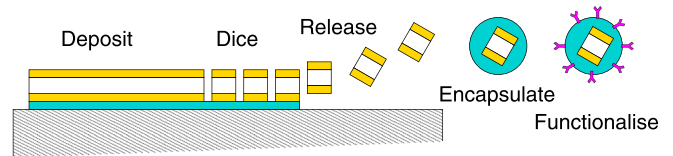
FIG. 7. (Color online) Schematic of the production process for transducers, showing deposition dicing and releasing of devices and future steps of encapsulation and functionalization.

of deposition we also measure the transmission spectra of white light through the structures and determine the layer thicknesses by comparison with Fresnel transmission coefficients.

This approach gives fine control of both the thicknesses and the overall device size. It allows easy monitoring of the devices and *in situ* measurements to be made before release to fine tune the design and fabrication process. However, the size and total number of devices made is limited, which in our case leads to a current minimum lateral device size of 5 μm over an area of a few cm^2 leading to the production of a few million devices per run. Obtaining a higher resolution mask and improving the exposure or using another machining technique such as focused ion beam or e-beam lithography will allow much smaller devices to be made.

The fabrication process is performed as follows: A cleaned glass substrate is coated with a thin polymer layer (PS dissolved in toluene) to act as a buffer layer for *in situ* testing and to be dissolved later to release the transducers into solution. Then a layer of photo resist is added, this is exposed to ultraviolet light through the optical mask with the device size of choice. The photoresist is then developed and the sandwich structure is then laid down using a sputter coater. The next stage is to lift off the remaining photoresist to leave the arrays of transducers on the substrate (see Fig. 8, left). The samples can then be measured *in situ* or the sacrificial PS layer can be dissolved by washing in toluene to leave the devices in solution for re-attachment—see Fig. 8.

The devices could then be encapsulated and/or functionalized. There are a number of different approaches to achieve this; one method is to make self-assembled monolayers (SAMs) on the metal surfaces of the transducer. SAM layers are a versatile coating as there is a wide variety of terminating functional groups which can be used to interact with a large number of molecules. This allows the SAM to
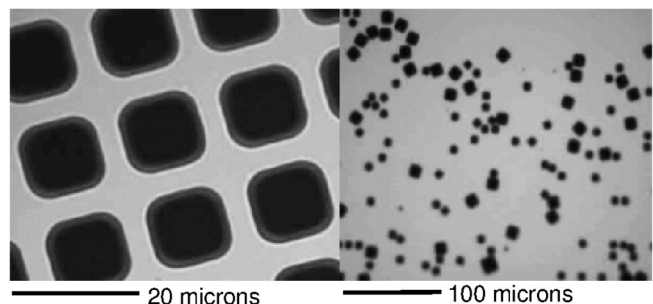

FIG. 8. Optical microscope image of (left) 15 μm lateral width transducers still *in situ* on the fabrication substrate and (right) liberated transducers in water (mixture of sizes 5 μm → 15 μm).

be tuned for different applications, for example, to become a bio-functional surface to interact with cells by selecting and attaching different types of proteins[31] or a smart surface having the initial surface properties of the formed film which changes in response to an external stimulus, e.g., chemical, optical, electric, or thermal.[32]

D. The design and fabrication of very small devices

The theory, modeling, and fabrication techniques used in Secs. II A–II C have all assumed devices with a lateral width and optical illumination width greater than the thickness of the transducer and greater than the optical wavelength. There is no fundamental limitation on the lateral size of the transducers but as the lateral size decreases beyond these limits the approach to the theory, modeling, and fabrication needs to take the finite size of the transducers into account. In this paper, the transducers presented fall outside this limit and can be safely considered "big" and a full discussion of the consideration needed for "small" devices is beyond the scope of this paper but it is worth considering the challenges:

(1) As the lateral size decreases below the optical spot size the optical cross section decreases, leading to a reduced coupling efficiency for generation and detection with an associated decrease in the signal-to-noise ratio.
(2) As the lateral size $\ll \lambda_{optical}$ the infinite plate model used to compute the Fresnel reflection coefficients is no longer valid. In particular the refractive index of the internal dielectric layer becomes less significant as the bulk of the optical energy carried between the metal "layers" is now carried in the external medium which will lead to a displacement of the optical resonances. Except for special geometries this requires 3D numerical modeling to predict the optical response.
(3) Any structure or illumination in the small limit can lead to the generation and detection of more complex mechanical resonant modes, for example, shear, surface, or edge resonances. These additional resonances have been observed in 3D finite element models and can considerably complicate the response of the transducer. Careful design will be required to limit their impact on the transducers' performance. However these additional modes may also be put to good use and may provide additional information about the transducer or environment.
(4) As the lateral size $\ll \lambda_{optical}$ photolithography techniques become increasingly difficult and expensive; however, as this occurs alternative techniques such as direct e-beam lithography, focused ion beam milling, and molecular self-assembly techniques become possible.[33]

III. EXPERIMENTAL TESTING OF TRANSDUCERS

A. Experimental setup

Figure 9 shows a simple schematic of the experimental system used to test the transducers. The experiment is based around a dual laser asynchronous optical sampling ASOPS system.[34–36] This controls two femto-second pulsed lasers
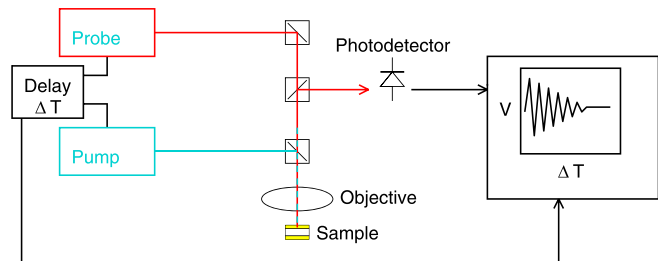
FIG. 9. (Color online) Schematic of the experimental system; the lasers are controlled using electronics that allows the delay between the pump and probe pulse to be set and swept. The system also incorporates an inline phase contrast microscope for simultaneously imaging the samples (not shown).

($\sim$150 fs pulse width) with repetition rates of $\sim$100 MHz and allows the delay between the pulses, ΔT, to be set and swept electronically at a relatively high speed. In our system the delay between the pump and probe pulses is swept from 0 to 10 ns every 100 μs (10 kHz).

The system uses a maximum of 4 mW average power in the probe (780 nm) and 1 mW in the pump (390 nm) corresponding to pulse energies of 40 and 10 pJ and peak powers of $\sim$240 and $\sim$60 W, respectively.

B. Transducer response

The response of the transducer is detected by monitoring the low frequency ($<$30 MHz) intensity variation of the probe light on a photo-detector and captured and averaged on a digital oscilloscope (DSO). The short pulses of the probe "strobe" the transducer and mix down the very high frequency (GHz) response of the transducer to a much lower frequency. With this arrangement a signal detected at a delay of T on the DSO corresponds to a real delay between the laser pulses (ΔT) of $T/10\,000$ and a frequency measured on the DSO of f_{scope} corresponds to a real frequency of $10\,000 f_{scope}$.

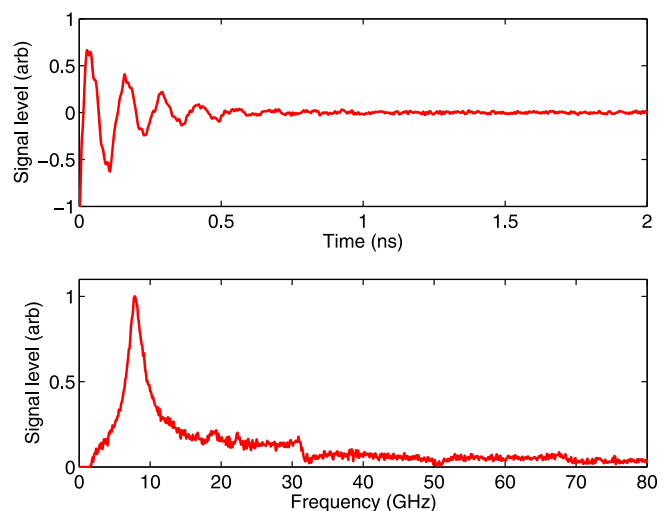As drawn in Fig. 9 the pump and probe beams are focused to the same location on the top of the transducer;

FIG. 10. (Color online) Experimentally measured time trace and spectrum obtained from a 5 μm transducer (compare with Fig. 4).
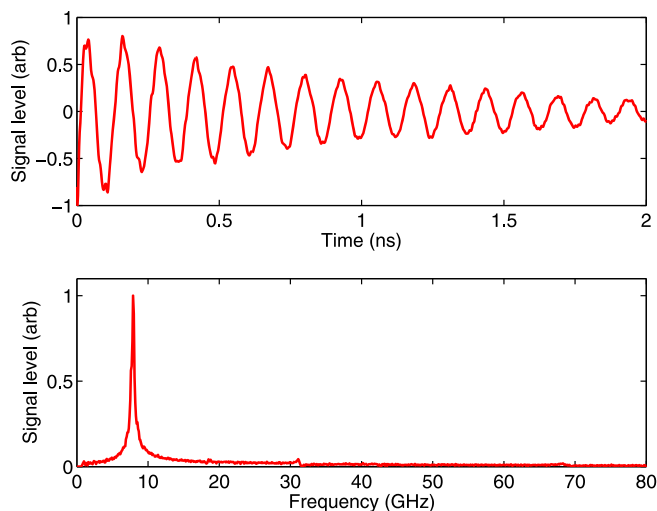
FIG. 11. (Color online) Experimentally measured time trace and spectrum obtained from a 5 μm transducer fabricated with an intermediate PS layer between it and the substrate (compare with Fig. 5).

however, the system allows for the beams to be separated in *x*, *y*, and *z* and to come from both sides of the sample if required.

The signals recorded on the DSO also contain a "coincidence peak" which occurs when the pump and probe pulses occur at the same time (which indicates $\Delta T = 0$) and a slow thermal decay. These are removed by subsequent signal processing to leave just the oscillatory signal corresponding to the mechanical response of the transducer.[27,28]

Figure 10 shows typical results obtained from a 10 μm transducer on top of a glass substrate. The gold layers were 30 and 32 nm thick and separated by a 160 nm layer of ITO. The measured signal is very similar to the modeled result presented in Fig. 4. The differences are likely due to slight variations in the actual layer thicknesses created and the mechanical properties of the materials differing from those published values used in the model.

Figure 11 shows the same for a transducer on top of a PS layer to provide acoustic isolation—this can be compared with the modeling result shown in Fig. 5. It can be seen that the *Q* of the resonance is increased because the losses through acoustic radiation are reduced. This shows that the transducers' response is closely coupled to the media they are attached to and that it is possible to manipulate the transducer through additional layers to control its bandwidth.

C. Application to the detection of protein

Figure 12 shows the ability of the transducers to sense the presence of other materials on the device. A large plate transducer was prepared by transfer stamping it with a 3% solution in water of bovine serum albumin (BSA) protein and drying to leave regions thinly coated with BSA. The sample was then inverted so that the transducer was excited and readout from underneath and the pump and probe beams did not pass through the protein layer (see Fig. 13).

An optical image was taken of the protein on the transducer simultaneously with the acoustic measurements (Fig. 12, bottom). By exciting and detecting the ultrasound
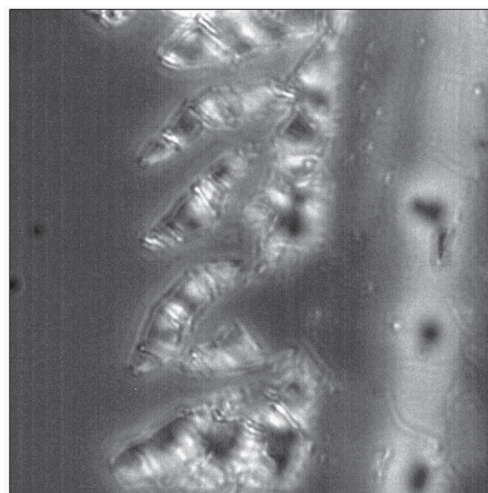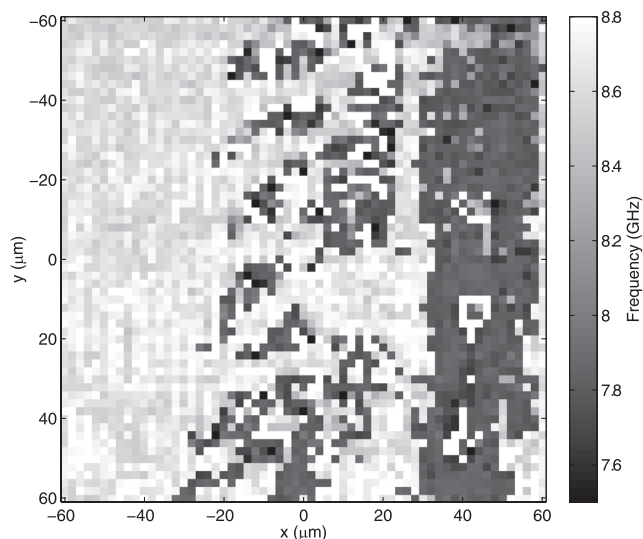

FIG. 12. (Top) Main resonant frequency of a sample with BSA protein deposited on the top surface of a large transducer. (Bottom) Microphotograph of the protein deposits roughly corresponding to the same area. The acoustic measurement was taken with the pump and probe light incident from the substrate side (below the protein coated surface). The two images are strongly correlated, demonstrating that the transducer is sensitive to the presence of the protein. This image took an average of 50 k signal at each point taking ∼30 s /point. The scanning speed is currently limited by the data acquisition system that can only capture ∼ 1/6 of the available data.

using small (∼2 μm) optical spots for the pump and probe beam and then scanning these spots it was possible to build up a map or image of the acoustic response. In Fig. 12, the region with no protein, the transducers' main resonance is ∼8.5 GHz but this is down-shifted to ∼7.8 GHz in the regions coated with protein as the additional mass of the protein adhered to the surface reduces the resonant frequency of the device. The shift in resonance frequency could be used to estimate the thickness of the protein layer. A simple simulation suggests that for a similar transducer a protein layer of ∼15 nm would lead to the observed shift of 700 MHz. This layer thickness is higher than expected for the protein stamping technique used on this sample but we can see from the optical image that the protein has clumped together during drying so the thicker value is not surprising. This was a crude test but it can be seen that the acoustic image matches the optical microscopy image taken of the protein on the top

J. Acoust. Soc. Am., Vol. 137, No. 1, January 2015

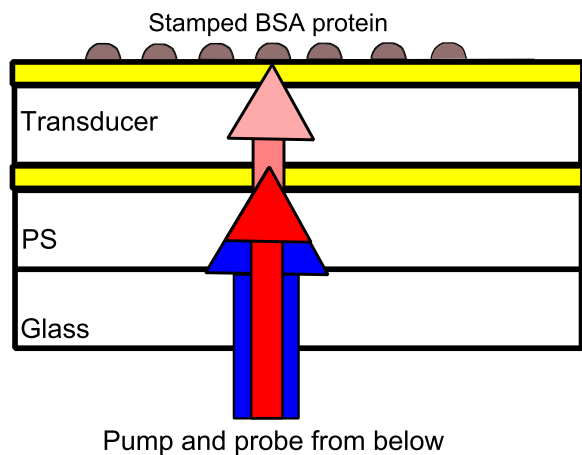Smith *et al.*: Optically excited ultrasonic transducers   225

FIG. 13. (Color online) A cartoon of the arrangement for the stamped BSA protein experiment: The pump and probe beams are both incident from below; the reflected probe light is directed to the detector so that it does not pass through the protein layer.

side of the transducer well and demonstrates the devices' sensitivity to the environment.

IV. DISCUSSION

In this paper we have demonstrated an optical ultrasonic transducer capable of generating and detecting high frequency ultrasound ($\sim$1–50 GHz) with wavelengths of the order and smaller than visible optical wavelengths. The design of the transducer exploits optical and mechanical resonances to achieve a good practical sensitivity. The experimentally measured transducers show good agreement with theory and modeling and experimental results showing sensitivity to external media and mass loading are demonstrated.

The fabrication techniques used currently limit the lateral size of the transducers to 500 nm but this is not a fundamental limit; however, as the devices get smaller than this limit the design and fabrication challenges increase.

There are a number of potential improvements that could enhance the performance of the devices. For example, the generation mechanism is currently based on the optical absorption of the metal films at λ_{pump} but as we typically use gold films it would be possible to enhance the absorption by utilizing surface plasmon polaritons. At the plasmon angle the absorption is greatly increased and would allow the generation of higher amplitude acoustic waves. The incident angle requirements are currently difficult to implement in our present instrument configuration so the magnitude of this improvement has not been investigated as yet.

The operating acoustic frequency range with an acceptable sensitivity range was discussed in Fig. 6; this showed that you can trade some sensitivity to tune to a specific acoustic frequency. However, if a tunable laser is available for the probe beam then there is much greater flexibility to tune the operating frequency and still maintain maximum sensitivity.

The optoacoustic transducers presented are simple to make and could be used in a wide variety of applications; by utilizing the generation and detection capabilities of arrays

of transducers many of the acoustic imaging modes performed at lower frequencies with piezoelectric transducers could be performed. This would allow, for example, 3D tomography and acoustic imaging of small features or samples. Using the devices for detection of acoustics waves generated through photoacoustic conversion of absorbers in a sample could allow photoacoustic imaging on the nanoscale. For this application to be realizable the acquisition speed would need to increase considerably; this could be achieved by the parallelization of the detection electronics, for example, by using a linear array of photodiodes and a fast multichannel channel data acquisition solution.

[1]B. Hadimioglu and C. F. Quate, "Water acoustic microscopy at suboptical wavelengths," Appl. Phys. Lett. **43**, 1006–1007 (1983).

[2]J. Heiserman, D. Rugar, and C. F. Quate, "Cryogenic acoustic microscopy," J. Acoust. Soc. Am. **67**, 1629–1637 (1980).

[3]P. A. Mante, J. F. Robillard, and A. Devos, "Complete thin film mechanical characterization using picosecond ultrasonics and nanostructured transducers: Experimental demonstration on SiO$_2$," Appl. Phys. Lett. **93**, 071909 (2008).

[4]P. Babilotte, P. Ruello, D. Mounier, T. Pezeril, G. Vaudel, M. Edely, J.-M. Breteau, V. Gusev, and K. Blary, "Femtosecond laser generation and detection of high-frequency acoustic phonons in GaAs semiconductors," Phys. Rev. B **81**, 245207 (2010).

[5]W. Chen, Y. Lu, H. J. Maris, and G. Xiao, "Picosecond ultrasonic study of localized phonon surface modes in Al/Ag superlattices," Phys. Rev. B **50**, 14506–14515 (1994).

[6]O. B. Wright, B. Perrin, O. Matsuda, and V. E. Gusev, "Optical excitation and detection of picosecond acoustic pulses in liquid mercury," Phys. Rev. B **78**, 024303 (2008).

[7]M. Ducousso, O. El-Farouk Zouani, C. Chanseau, C. Chollet, C. Rossignol, B. Audoin, and M.-C. Durrieu, "Evaluation of mechanical properties of fixed bone cells with sub-micrometer thickness by picosecond ultrasonics," European Phys. J. Appl. Phys. **61**, 11201–11211 (2013).

[8]T. Dehoux and B. Audoin, "Non-invasive optoacoustic probing of the density and stiffness of single biological cells," J. Appl. Phys. **112**, 124702 (2012).

[9]T. Dehoux, T. A. Kelf, M. Tomoda, O. Matsuda, O. B. Wright, K. Ueno, Y. Nishijima, S. Juodkazis, H. Misawa, V. Tournat, and V. E. Gusev, "Vibrations of microspheres probed with ultrashort optical pulses," Opt. Lett. **34**, 3740–3742 (2009).

[10]D. Segur, Y. Guillet, and B. Audoin, "Intrinsic geometric scattering probed by picosecond optoacoustics in a cylindrical cavity: Application to acoustic and optical characterizations of a single micron carbon fiber," Appl. Phys. Lett. **97**, 031901 (2010).

[11]T. A. Kelf, Y. Tanaka, O. Matsuda, E. M. Larsson, D. S. Sutherland, and O. B. Wright, "Ultrafast vibrations of gold nanorings," Nano Lett. **11**, 3893–3898 (2011).

[12]J. Aizpurua, G. W. Bryant, L. J. Richter, F. J. Garca de Abajo, B. K. Kelley, and T. Mallouk, "Optical properties of coupled metallic nanorods for field-enhanced spectroscopy," Phys. Rev. B **71**, 235420 (2005).

[13]D. Mongin, V. Juve, P. Maioli, A. Crut, N. Del Fatti, F. Vallee, A. Sanchez-Iglesias, I. Pastoriza-Santos, and L. M. Liz-Marzan, "Acoustic vibrations of metal-dielectric core-shell nanoparticles," Nano Lett. **11**, 3016–3021 (2011).

[14]H.-Y. Chiu, P. Hung, H. W. C. Postma, and M. Bockrath, "Atomic-scale mass sensing using carbon nanotube resonators," Nano Lett. **8**, 4342–4346 (2008).

[15]J. N. Anker, W. P. Hall, O. Lyandres, N. C. Shah, J. Zhao, and R. P. Van Duyne, "Biosensing with plasmonic nanosensors," Nat. Mater. **7**, 442–453 (2008).

[16]A. Campion and P. Kambhampati, "Surface-enhanced Raman scattering," Chem. Soc. Rev. **27**, 241–250 (1998).

[17]H. Xu, J. W. Aylott, R. Kopelman, T. J. Miller, and M. A. Philbert, "A real-time ratiometric method for the determination of molecular oxygen inside living cells using sol-gel-based spherical optical nanosensors with applications to rat C6 glioma," Anal. Chem. **73**, 4124–4133 (2001).

[18]P. G. Coupland, S. J. Briddon, and J. W. Aylott, "Using fluorescent ph-sensitive nanosensors to report their intracellular location after Tat-mediated delivery," Integr. Biol. **1**, 318–323 (2009).

[19]J. D. Hamilton, T. Buma, M. Spisar, and M. O'Donnell, "High frequency optoacoustic arrays using etalon detection," IEEE Trans. Ultrason., Ferroelectr. Freq. Control **47**, 160–169 (2000).

[20]M. Born and E. Wolf, *Principles of Optics*, 7th ed. (Cambridge University Press, Cambridge, 1999), 367 pp.

[21]S.-W. Huang, Y. Hou, S. Ashkenazi, and M. O. Donnell, "High-resolution ultrasonic imaging using an etalon detector array," Appl. Phys. Lett. **93**, 113501 (2008).

[22]E. Z. Zhang and P. C. Beard, "A miniature all-optical photoacoustic imaging probe," in *Photons Plus Ultrasound: Imaging and Sensing* (SPIE, Bellingham, WA, 2011), Vol. 78991F.

[23]Y. Li, Q. Miao, A. Nurmikko, and H. Maris, "Picosecond ultrasonic measurements using an optical cavity," J. Appl. Phys. **105**, 083516 (2009).

[24]R. Smith, A. Arca, X. Chen, L. Marques, M. Clark, J. Aylott, and M. Somekh, "Design and fabrication of ultrasonic transducers with nanoscale dimensions," J. Phys. Conf. Ser. **278**, 012035 (2011).

[25]R. Smith, A. Arca, X. Chen, L. Marques, M. Clark, J. Aylott, and M. G. Somekh, "Design and fabrication of nanoscale ultrasonic transducers," J. Phys. Conf. Ser. **353**, 012001 (2012).

[26]P. Morris, A. Hurrell, A. Shaw, E. Zhang, and P. Beard, "A Fabry–Pérot fiber-optic ultrasonic hydrophone for the simultaneous measurement of temperature and acoustic pressure," J. Acoust. Soc. Am. **125**, 3611–3622 (2009).

[27]O. Matsuda, O. B. Wright, D. H. Hurley, V. E. Gusev, and K. Shimizu, "Coherent shear phonon generation and detection with ultrashort optical pulses," Phys. Rev. Lett. **93**, 095501 (2004).

[28]D. Hurley, O. Wright, O. Matsuda, V. Gusev, and O. Kolosov, "Laser picosecond acoustics in isotropic and anisotropic materials," Ultrasonics **38**, 470–474 (2000).

[29]O. Matsuda and O. B. Wright, "Reflection and transmission of light in multilayers perturbed by picosecond strain pulse propagation," J. Opt. Soc. Am. B **19**, 3028–3041 (2002).

[30]ITO is conductive at sub-optical frequencies and can easily be DC sputtered whereas insulators such as SiO_2 cannot be.

[31]M. Frasconi, F. Mazzei, and T. Ferri, "Protein immobilization at gold-thiol surfaces and potential for biosensing," Anal. Bioanal. Chem. **398**, 1545–1564 (2010).

[32]P. Mendes, "Stimuli-responsive surfaces for bio-applications," Chem. Soc. Rev. **37**, 2512–2529 (2008).

[33]R. D. Averitt, S. Westcott, and N. J. Halas, "Linear optical properties of gold nanoshells," J. Opt. Soc. Am. B **16**, 1824–1832 (1999).

[34]P. A. Elzinga, F. E. Lytle, Y. Jian, G. B. King, and N. M. Laurendeau, "Pump/probe spectroscopy by asynchronous optical sampling," Appl. Spectrosc. **41**, 2–4 (1987).

[35]A. Bartels, R. Cerna, C. Kistner, A. Thoma, F. Hudert, C. Janke, and T. Dekorsy, "Ultrafast time-domain spectroscopy based on high-speed asynchronous optical sampling," Rev. Sci. Instrum. **78**, 035107 (2007).

[36]V. A. Stoica, Y.-M. Sheu, D. A. Reis, and R. Clarke, "Wideband detection of transient solid-state dynamics using ultrafast fiber lasers and asynchronous optical sampling," Opt. Express **16**, 2322–2335 (2008).